Quantum mechanical tunneling of composite particle systems: Linkage to sub-barrier nuclear reactions

A. C. Shotter[1] and M. D. Shotter[2,*]

[1]*School of Physics and Astronomy, University of Edinburgh, Edinburgh, United Kingdom and TRIUMF, Vancouver, Canada*

[2]*Department of Physics, University of Oxford, Oxford, United Kingdom*

(Received 8 February 2011; published 31 May 2011)

A variety of physical phenomena have at their foundation the quantum tunneling of particles through potential barriers. Many of these phenomena can be associated with the tunneling of single inert particles. The tunneling of composite systems is more complex than for single particles due to the coupling of the tunneling coordinate with the internal degrees of freedom of the tunneling system. Reported here are the results of a study for the tunneling of a two-component projectile incident on a potential energy system which differs for the two components. A specific linkage is made to sub-Coulomb nuclear reactions.

DOI: 10.1103/PhysRevC.83.054621 PACS number(s): 25.60.Pj, 25.60.Gc, 03.65.Nk, 03.65.Xp

I. INTRODUCTION

A wide range of physical phenomena and many related applications have at their foundation some aspect of quantum particle tunneling. The chemical elements of stars, radioactivity, chemical reactions at low energy, tunnel diodes, Josephson junctions, scanning tunneling microscopes, and scanning probe position encoders, to name a few, have an origin based on quantum tunneling [1,2]. These processes can usually be well described by the transmission of single or tightly bound composite particles. For this reason a large body of tunneling literature relates to one-dimensional tunneling of single inert units.

In nuclear physics quantum tunneling plays a vital role in the phenomena of fission, sub-Coulomb reactions, and radioactivity. Nuclear reaction models, which are used to parametrize such phenomena, are often based on a single-coordinate tunneling formalism, with the addition that either or both of the reacting nuclei can be excited to various states. This approach has been particularly successful when interpreting fusion of stable nuclei at or below the Coulomb barrier. More recently sub-Coulomb nuclear reactions are being studied for situations in which one of the participant nuclei is short lived, i.e., radioactive. While studies with radioactive beams are of interest in their own right, they also have relevance for the production of very heavy elements and to astrophysical situations such as supernovae and other explosive scenarios.

Sub-Coulomb fusion reactions involving radioactive nuclei have been discussed in the literature for a number of years, but as yet there is no consensus as to the relative importance of the different physical processes thought to be involved. There are even different views as to whether a particular physical effect will enhance or suppress the fusion probability. Part of the problem is that due to the low intensity of radioactive beams, measurements of such reactions are very challenging; as a consequence the database is still quite sparse. Another problem is that the theoretical description of such fusion reactions is very challenging due to the complexity of competing physical processes.

There have been various experimental fusion studies with radioactive beams, for example, ^{6}He [3–8], ^{11}Be and ^{10}Be [9–11], and ^{8}Li [12]. Due to the difficulty in using radioactive beams, various fusion studies have in addition been undertaken recently using weakly bound stable light-ion beams, for example, ^{6}Li and ^{7}Li [13–15] and ^{9}Be [16]. The interpretation of the fusion data, and its implication for quantum tunneling of nuclei, has centered on four main areas of interest:

(i) the extended neutron radial distribution of neutron-rich nuclei, and how this could lead to a lowering of the Coulomb barrier and so enhance the fusion probability;
(ii) the presence of possible soft resonances associated with the extended neutron tail of neutron-rich nuclei;
(iii) the low neutron binding of neutron-rich nuclei, and how this can lead to breakup of the projectile into the continuum; and
(iv) transfer of the weakly bound outer neutrons of neutron-rich nuclei to deeper binding states in the target.

A brief referenced discussion of these four areas of interest follows below. Concerning (i), Canto *et al*. [17] have recently emphasized that when comparing the fusion of different neutron-rich isotopes it is important to separate out the static effects of the extended neutron tail so that possible dynamic effects can be isolated. The physical situation associated with (ii) is of an extended neutron tail resonating with the charged core of a neutron-rich nucleus, producing a low-energy giant resonance that could be excited in a collision and lead to an enhanced fusion cross section [18–20].

The picture that is emerging from (iii) is less clear. It has been argued that the breakup should be treated as any other channel that couples into the entrance channel, i.e., it should lead to an enhancement of fusion in the sub-Coulomb energy region [21–26]. However, other calculations indicate that breakup can lead to a reduction in the complete fusion cross section in the sub-Coulomb region, since there is a

*Secondary affiliation: Atomic Physics Division, National Institute of Standards and Technology, Gaithersburg, MD 20899-8420.

significant chance that only part of the projectile will fuse with the target if the projectile dissociates before fusing [18–20,27]. This breakup process becomes more important the lower the binding energy of the projectile, and the higher the Z of the target, due to the process of Coulomb breakup [13,15,28].

The physical aspect associated with (iv) above has been reported in a series of papers [29–31]; these articles were inspired by a comparative study of sub-Coulomb fusion cross sections for ^{40}Ca+^{48}Ca and ^{48}Ca+^{48}Ca by Trotta *et al*. [32]. The idea put forward in these articles is that the increased fusion cross section for ^{40}Ca+^{48}Ca compared to ^{48}Ca+^{48}Ca is due to the transfer of neutrons from ^{48}Ca to ^{40}Ca, resulting in a conversion of neutron binding energy to the kinetic energy of the charged components and so increasing the likelihood of tunneling through the Coulomb barrier. This type of analysis was subsequently applied to a comparison of the fusion cross sections for ^{6}He and ^{4}He projectiles [8]; the hypothesis is that when two projectiles approach each other with a kinetic energy lower than the barrier, a positive Q value for neutron transfer will aid the charged cores to penetrate the barrier. However, it has also been reported elsewhere that the reverse should happen [33].

This experimental and theoretical work indicates that there is still considerable uncertainty concerning the physical processes and their relative importance to the fusion of neutron-rich unstable nuclei, especially at energies below the Coulomb barrier. This is due not only to the complexity of the tunneling process, but also to the current sparsity of experimental data, and to theoretical approaches which focus by necessity on a particular aspect of a reaction, making it difficult to draw general conclusions. The aim of the present paper is therefore to examine the tunneling problem using simple quantum models to investigate whether, even at this level of detail, general trends can be identified which find their expression in the full complexity of the tunneling of weakly bound unstable nuclei.

In his book on quantum tunneling Razavy [34] notes that, while the general literature on single-particle tunneling is extensive, there has been much less attention paid to the tunneling of composite particles. However, there have been a few studies that describe very interesting effects associated with the resonant tunneling of simple composite systems. Saito and Kayanuma [35] were the first to study the tunneling of a two-component system, for example, a diatomic molecule, through a one-dimensional barrier. Remarkable resonances were discovered that were attributed to the trapping of the molecule by the barrier, illustrating how the transmission of a projectile can be heavily influenced by its internal structure. This system was further investigated by Pen'kov [36,37] and later by Goodvin and Shegelski [38,39]. A related system was studied by Bonini *et al*. in the context of high-energy particle collisions [40]. More recent studies of tunneling have investigated a basic two-component system and its relation to the nuclear case [41,42].

Lee and Takigawa [43] investigated the time evolution of quantum tunneling for multidimensional systems by using path integral methods. This study in particular illustrates the intricate effects of the interplay between the tunneling and internal projectile degrees of freedom.

These studies of simple composite projectile tunneling are of interest but have limited capability to address the subject areas (i)–(iv) identified above, since in these theoretical studies only common external potentials are experienced by the projectile components, and no account is taken of projectile breakup. The main objective of this paper is to remove these limitations in order to establish if general insights for the nuclear case can be gained by a numerical study of two-component projectile systems tunneling through a two-component external potential.

II. THE REACTION MODEL

Previous studies of two-component projectiles tunneling through a barrier have demonstrated that the transmission coefficient can exhibit resonances as a function of projectile incident energy. The resonances are associated with the trapping of composite particles by the barrier; these are metastable situations in which one component has penetrated the barrier while still being attached to the other component which has yet to penetrate [35–38]. These studies express the time-independent projectile wave function as a functional series in the eigenfunctions of the unperturbed bound composite projectile; no account is taken of projectile breakup.

The study reported in this paper examines a two-component projectile incident on a potential system, using a method that allows for breakup of the projectile. The physical system is shown diagrammatically in Fig. 1. The two-component projectile is bound with a finite binding energy by the interaction V_{12}. The projectile in its ground state is incident on a fixed potential system $V_1(x_1)+V_2(x_2)$, with projectile component C_1 only interacting with $V_1(x_1)$ and component C_2 only interacting with $V_2(x_2)$. To allow for breakup, which involves a continuous spectrum of states, it was decided to investigate the collision by solution of the time-dependent Schrödinger equation rather than by the time-independent approach.

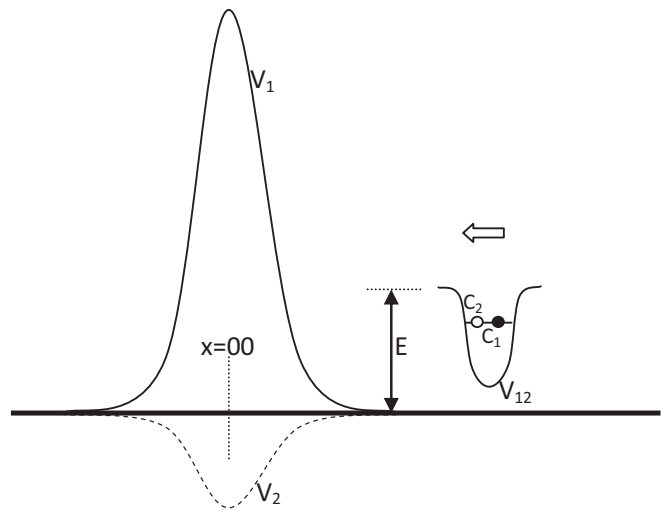

FIG. 1. Diagrammatic representation of the scattering system.

The functional forms for the projectile and potential system were chosen as

$$V_1(x_1) = V_{0(1)} \exp\left[-\left(\frac{x_1 - 30}{2.4}\right)^2\right],$$

$$V_2(x_2) = V_{0(2)} \exp\left[-\left(\frac{x_2 - 30}{2.4}\right)^2\right],$$

$$V_{12}(x_{12}) = \left(-V_{0(12)} + 0.3x_{12}^2\right) \Big/ \left[1 + \exp\left(\frac{|x_{12}| - 2}{0.1}\right)\right],$$

$$\psi(x_1, x_2, t = 0) = \exp[iK(x_1 + x_2)] \times \exp\left[-0.002\left(\frac{x_1 + x_2}{2} - x_{0(12)}\right)^2\right] \times f_{12}(x_{12}, V_{0(12)}).$$

Here, x_i is the position of component C_i, $x_{0(12)}$ is the center-of-mass position of the projectile when $t = 0$, and $x_{12} = x_1 - x_2$. The function f_{12} is the ground-state wave function calculated for the potential $V_{12}(x_{12})$, and ψ is the projectile wave function at $t = 0$. The units used throughout this paper are MeV for energy, 10^{-15} m = 1 fm for distance, and 10^{-21} s = 1 zs for time. The barrier height $V_{0(1)}$ is fixed at 25 MeV; $V_{0(2)}$ is varied from 0 to −20 MeV. These two barriers are fixed in position 30 fm from the coordinate origin, near the center of the spatial grid (see Fig. 2 and Sec. III). The masses of the projectile components are both 1 amu, so in these units the momentum K is $(0.024E)^{0.5}$ fm^{-1}, where E is the projectile energy.

The parameters were chosen to be broadly characteristic of light nuclei sub-barrier reactions. The forms of V_1 and V_2 were chosen as Gaussian to be similar to previous composite projectile calculations [36–38,40,41]. The parameters of the initial wave packet were chosen such that it had negligible overlap with the fixed potential system. Reaction outcomes were studied for a range of values for $V_{0(2)}$, projectile binding potential parameter $V_{0(12)}$, and initial projectile kinetic energy E.

III. NUMERICAL SOLUTION OF THE TIME-DEPENDENT SCHRÖDINGER EQUATION

The primary objective of the calculation was to determine the final outcomes of the reactions, so each calculation was run until the entire wave packet left the interaction region in order to allow accurate extrapolation to the asymptotic (long-time) solution. The spatial coordinate ranges were chosen to ensure that reflections at the boundaries of the numerical grid did not interact again with the central potential. The accuracy of the calculation could have been increased by using a larger spatial grid at the cost of increased computational overhead; a compromise was chosen to balance accuracy and

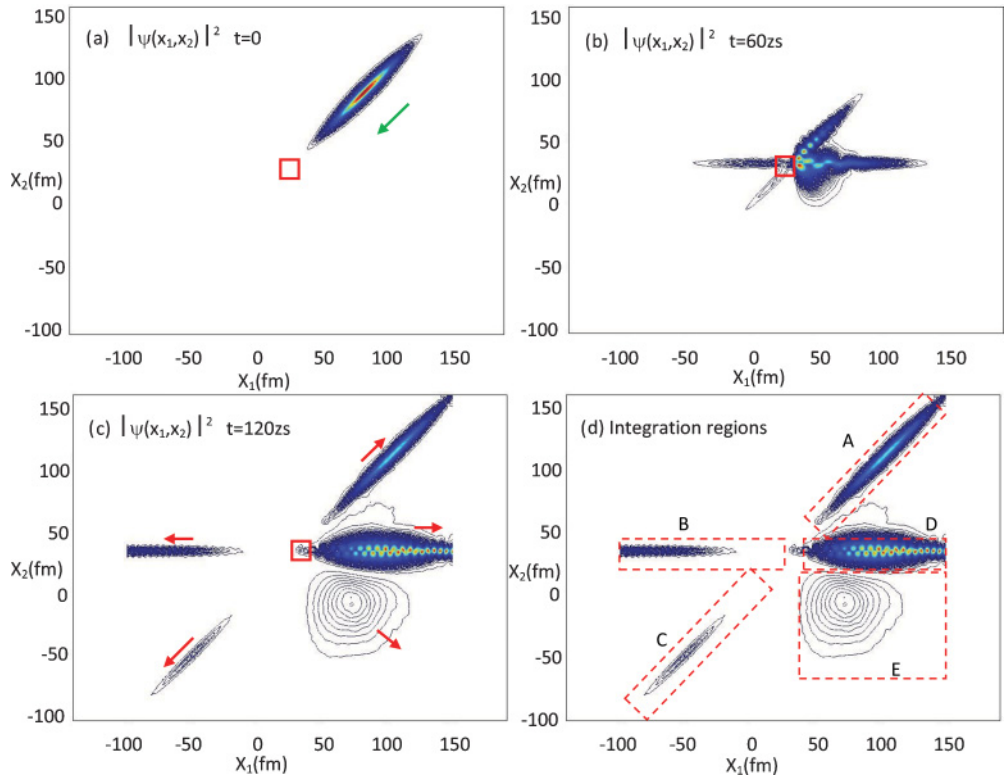

FIG. 2. (Color online) Illustration of the collision and the different reaction outcomes. The central red box indicates the region in which both components are in contact with the scattering potential. The reaction outcomes associated with regions A-E are discussed below.

computational time. The coordinate space for both x_1 and x_2 ranged from -100 to 150 fm, with the initial center of mass of the composite projectile at 80 fm. The spatial grid mesh in the plane (x_1, x_2) was refined until the normalization of the wave function could be maintained within a band of $1\pm(2\times10^{-8})$ for the time span of the calculation. The differential equation kernel within the Comsol multiphysics software was used to solve the time-dependent Schrödinger's equation.

IV. CHARACTERIZATION OF SCATTERING AMPLITUDE

Figures 2(a)–2(c) show contour plots of the probability amplitude $|\Psi(x_1, x_2)|^2$ at times 0, 3, and 6 zs for typical parameters. It can be seen that a particularly valuable feature of the time-dependent calculation is the insight it provides into how the continuous evolution of the initial wave packet relates to the final outcome.

In order to quantify the outcomes, the coordinate plane (x_1,x_2) is divided into different regions as indicated in Fig. 2(d). After the interaction, region A corresponds to elastic scattering; C corresponds to transmission of the bound composite system; B corresponds to transmission of C_1 with capture of C_2 in the potential well V_2; D corresponds to reflection of C_1 with capture of C_2 in the potential well V_2, and E corresponds to breakup of the composite projectile with both components moving away from the scattering potential. Breakup flux into other regions is generally negligible when compared to region E.

Reaction probabilities are calculated as the integrated values of the probability for particular reaction outcomes; for example, the elastic scattering probability is calculated by the integration $\int_A |\Psi(x_1, x_2)|^2\, dx_1\, dx_2$ over region A of Fig. 2(d). Some uncertainly will be inherent in assigning the integrated probability in any region to a particular physical process due to spreading of the wave function from neighboring regions. Therefore, even though the total probability normalization is within $1\pm(2\times10^{-8})$ over the full coordinate space, the accuracy of assigning asymptotic probabilities within regions A–E to particular processes may have relative uncertainties of several percent.

V. ASYMPTOTIC REACTION PROBABILITIES

A. General comments

First consider the physical outcomes of the system shown in Fig. 1 under limiting conditions for the binding of the projectile components. If the coupling constant ω in $V_{12} = \omega(x_1 - x_2)^2$ is large, then $x_1 \approx x_2$ and the composite particle will interact as a single unit encountering a common potential $V_1(x) + V_2(x)$. At large ω and for a given projectile energy, as the potential V_2 becomes more negative, the transmission of the unit through the potential system will increase. In the other limit $\omega\to0$, the two particles will act independently, with each separately interacting with $V_1(x_1)$ or $V_2(x_2)$ and either being reflected or transmitted at the barrier; each particle has a total energy $E/2$ throughout the collision, as energy cannot be transferred between the particles. The interest in the current investigation is to consider the intermediate situation where there is a finite coupling between C_1 and C_2, with the possibility that C_2 can become bound in V_2.

The various reaction outcomes have been calculated as a function of the projectile kinetic energy E and the Q_g value. The Q_g value is defined as $B_2 - B_{12}$, where B_2 is defined as the ground-state binding of component C_2 in the potential well $V_2(x_2)$, and B_{12} is the ground-state binding of C_2 in the projectile. The reaction probabilities for different Q_g values were determined first by running calculations for different values of $V_{0(2)}$ ranging from 0 to -20 MeV.

B. Reaction outcomes involving reflection of C_1 by V_1

The probabilities for projectile elastic scattering and C_2 capture by V_2 are shown in Fig. 3. The general trend of these curves is similar between Figs. 3(a) and 3(b) but with the probabilities inverted, i.e., the probability is a maximum for Q_g values near zero for Fig. 3(b) and minimum for Fig. 3(a).

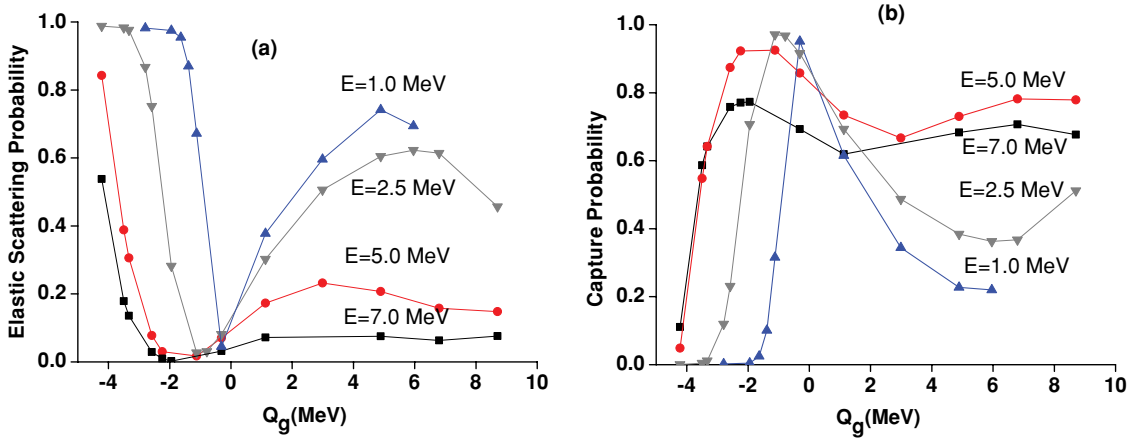

FIG. 3. (Color online) Figure (a) shows the asymptotic integrated value of the probability for elastic scattering as a function of Q_g for different values of the projectile energy E. Figure (b) corresponds to the asymptotic probability of region D of Fig. 2(d), i.e., capture of C_2 in V_2 and reflection of C_1 by V_1. For both Figs. (a) and (b), Q_g was varied by changing B_2, the binding of component C_2 in the potential well V_2.

For the two limiting situations discussed in Sec. V A, capture of C_2 would not be possible, so the capture functions of Fig. 3(b) can be directly attributed to the finite coupling between C_2 and C_1. This means that the projectile, upon interaction with V_1+V_2, can exchange energy between C_2 and C_1, and in particular C_2 can be captured in V_2, with the balance of energy being transferred to C_1. If $Q_g<0$, then capture of C_2 will reduce the kinetic energy available to C_1. For $Q_g>0$, C_2 is more bound in V_2 than in V_{12} so this extra binding will increase the kinetic energy available to C_1.

Away from $Q_g=0$, there is a decrease in elastic probability and an increase in reaction probability for increasing E. This behavior is to be expected on an intuitive level; the harder the projectile hits, the more likely an inelastic reaction will occur. However, the behavior around $Q_g\sim0$ is dominated for all energies E by a minimum in the elastic reflection probability and by a maximum in the reaction probability; this behavior becomes more pronounced as the projectile energy decreases. This maximum and minimum behavior may be understood by the following discussion. As the projectile's wave function overlaps the external potential system (Fig. 1), C_2 can be transferred to V_2; the transference probability will depend on the relative binding energy of C_2 in V_2 compared to that of C_2 in V_{12} (the difference between these two energies is the Q_g value). The greater the difference between these two energies, the greater will be elastic scattering rather than transfer. The situation is similar to that of the classic case of a single particle incident on a potential step, where starting with complete transmission for a zero-height potential step, the transmission decreases as the magnitude of the step size increases. It is suggested here that Q_g for the two-particle system of Fig. 1 has the same role to the potential step for the one-particle scattering situation. For the situation illustrated in Fig. 1, the maximum transference region would be expected to move to negative Q_g values to ensure that as the kinetic energy E of the bound projectile increases, the energy difference between the two well energies for C_2 (taking full account of E) is a minimum. Of course, the situation is made more complicated due to the interaction of C_1 with V_1, which rapidly changes with separation and therefore the interaction between the two wells.

For higher values of E the capture probability again increases for higher Q_g [Fig. 3(b)]. This is associated with capture of C_2 into the first excited state in V_2; this state is bound for $V_2<-12$ MeV (note: $Q_g=2.7$ MeV at $V_2=-12$ MeV). As an illustration of this behavior, the data shown in Fig. 2 is for $E=5$ MeV and $V_2=-15$ MeV; the double-node oscillatory structure of the first excited state of C_2 in V_2 (region D) can be seen clearly.

C. Reaction outcomes involving the transmission of C_1 through V_1

Figure 4 shows the asymptotic values of the transmission probability for the tunneling of C_1, where C_2 is either trapped in V_2 [region B, Fig. 2(d)] or is transmitted bound to C_1 [region C, Fig. 2(d)], as a function of Q_g and for different values of the projectile energy E.

The first case will be designated by TC (transmission-capture), and the second by TT (transmission-transmission). There are several interesting features of these transmission functions: (a) For negative Q_g values, the probability P(TT) for the outcome TT is greater than the probability P(TC) for the outcome TC, i.e., P(TT)>P(TC); (b) for positive Q_g values, P(TC)>P(TT); and (c) for all projectile energies E investigated, P(TT) and P(TC) are equal (the curves cross) at a point near $Q_g=0$.

Feature (c) could be an important clue to the physics associated with Fig. 4. Some years ago Pruess and Lichtner [44] argued that when interpreting "slow" nucleus-nucleus collisions it is important to take into account the effect of the internal particle states continuously adjusting to the instantaneous potential between the two closing nuclei. The authors referred to this distortion of the states as "shape polarization." For the case of a reaction involving the transfer of a nucleon between the two nuclei, a special case arises at $Q_g\approx 0$. In this situation the nucleon undergoes a tunneling process between the nuclei with a characteristic transfer time of $(\pi/2)\hbar/|H_{12}|$, where $|H_{12}|$ is the off-diagonal energy matrix element of the two-center nuclear system. If this cycle time is sufficiently short then several population cycles can occur as the nuclei are close—a situation termed resonant polarization by Pruess and Lichtner. For the present situation specified in Fig. 1 and Sec. II, $(\pi/2)\hbar/|H_{12}|\approx 0.3\times10^{-21}$ s at 5-fm separation, and 1.3×10^{-21} s at 10-fm separation; these times are independent of projectile energy. It therefore could be argued that resonance polarization is the reason why there is equal probability for TT and TC at $Q_g\approx 0$ since in this condition C_2 can easily pass between V_1 and V_2.

A possibly more illuminating way of describing this is that the transmission of C_1 through the barrier V_1 is necessarily accompanied by a transitory situation in which C_1 and C_2 are both approximately coincident with the barrier. As C_1 tunnels through the barrier and begins to depart the barrier region, the component C_2 experiences a diverging double-well potential, with one well centered on the barrier, and one well centered on C_1. In the moments immediately following the tunneling event there is a "tug of war" between the component C_1 and the barrier over which ends up with the component C_2. The wave function of the component C_2 continuously reacts to the combined potential; although one may imagine details such as a sloshing oscillation between the two potential wells, overall one would predict that the deeper well, i.e., the well which can exert the greater force on the component C_2, will gain the majority of the C_2 wave function. This can be seen in features (a) and (b) listed above. When the two wells have the same depth, so each exert around the same force on the component C_2, the division of the C_2 wave function between the potential V_2 and the component C_1 is approximately equal, as evidenced by feature (c).

Figure 5 shows the combined probability P(TT)+P(TC) for the transmission of C_1 through the barrier V_1. The formula $P\,(\mathrm{TT})+P\,(\mathrm{TC})=8.44\times10^{-5}\exp(0.33Q_g+0.88E-0.04E^2)$ can be used to parametrize the linear portion of these natural log curves. The appropriate curves using this parameterization are plotted in Fig. 5.

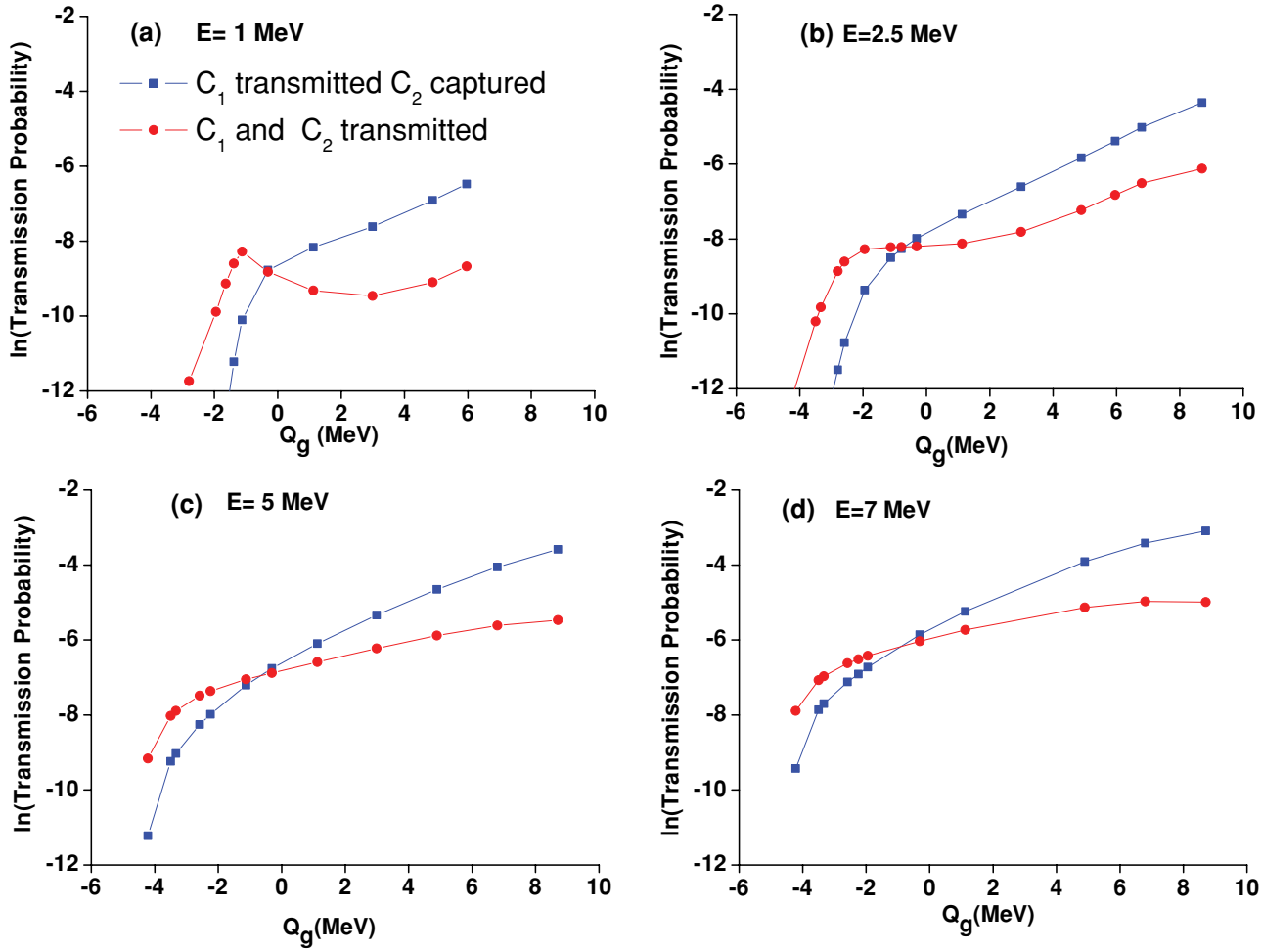

FIG. 4. (Color online) Transmission of C_1 with and without C_2; data point assignation shown in (a) also applies to (b), (c), and (d). For Figs. (a)–(d), Q_g was varied by changing B_2, the binding of component C_2 in the potential well V_2.

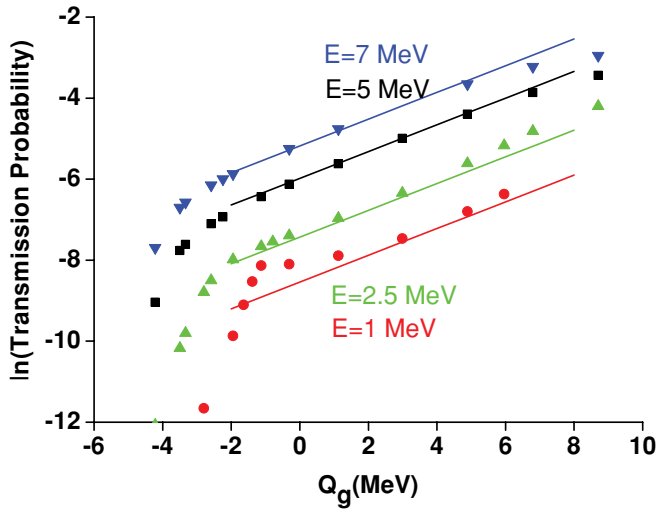

FIG. 5. (Color online) Combined transmission of C_1, $P(\mathrm{TC})+P(\mathrm{TT})$, for various projectile energies E. For this figure, Q_g was varied by changing B_2, the binding of component C_2 in the potential well V_2.

D. Influence of projectile breakup on other reaction processes

Figure 6(a) shows the variation of elastic scattering probability with projectile energy for three values of Q_g. For all Q_g values, the probability decreases with increasing projectile energy since at higher energy the projectile has greater ability to penetrate the potential. Figure 6(b) shows the probability for C_2 capture and C_1 reflection as a function of energy for the same three Q_g values; as expected, this probability initially increases with energy due to the increase in penetration with energy. However, the energy dependence shown in Fig. 6(b) changes for projectile energies greater than ∼4 MeV. To provide some insight into this effect, also plotted in Fig. 6(b) is the breakup probability of the projectile, which is the total integrated probability in region E of Fig. 2(d); it is seen that this probability increases significantly beyond 4 MeV. For the parameters used to calculate the data shown in Fig. 6, the binding energy of C_1 and C_2 interacting through V_{12} is 4.22 MeV; this value is indicated by the vertical dashed line in these plots. Breakup is not possible unless the projectile energy is greater than this energy. A loss of flux to the capture channel, and possibly even the elastic channel, can therefore be attributed to the increase in the probability flux to the breakup channel as the projectile energy increases.

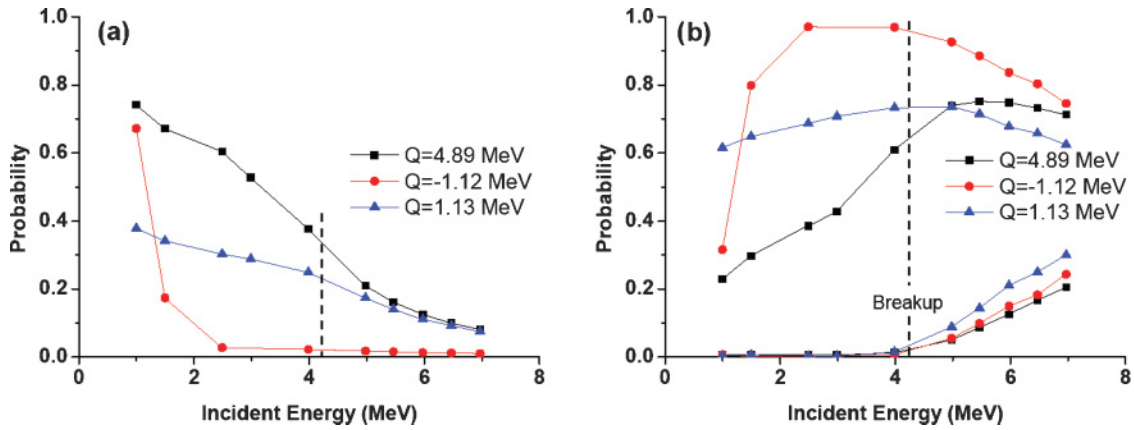

FIG. 6. (Color online) (a) Elastic scattering as a function of projectile energy and for different Q_g values, and (b) capture and breakup probabilities. Vertical lines indicate projectile breakup energy. For both Figs. (a) and (b), Q_g was varied by changing B_2, the binding of component C_2 in the potential well V_2.

Figure 7(a) shows probabilities for the transmission and breakup outcomes for Q_g=1.13 MeV as a function of the projectile kinetic energy. There appears to be a small change in the slope of the ln[P(TT)] curve at around the binding energy (4.22 MeV). We hypothesize that this decrease in the gradient of the transmission probability is related to the breakup process diverting flux away from the other reaction channels.

In order to investigate this hypothesis, data is shown in Fig. 7(b) for the same situation as in Fig. 7(a), but with a reduced projectile binding energy of 3 MeV, which increases Q_g to 2.34 MeV. The change in the slope of the transmission curves is shifted to ∼3 MeV, consistent with the hypothesis.

Note that the finite spatial width of the incident projectile wave packet gives it a kinetic energy width of ∼1 MeV. This acts to smear out sharp features in the plots, and accounts for effects such as the small probability of breakup for projectiles with a nominal kinetic energy a little less than their binding energy.

To further investigate the influence of projectile binding on reaction outcomes, data is shown in Fig. 8 for a projectile with kinetic energy 2.5 MeV and a range of projectile binding energies. From Fig. 8(a) it can be seen that the breakup probability becomes large when the binding energy is less than the kinetic energy of the projectile; this is accompanied by a corresponding reduction in the elastic scattering probability. However, the C_2 capture probability smoothly passes through the threshold breakup value without any obvious effect. Figure 8(b) shows the total transmission probability for C_1 to penetrate the V_1 barrier, i.e. P(TT)+P(TC). The two straight lines highlight the change in transmission at ∼2.5 MeV. The transmission probability becomes smaller as the binding energy is decreased, and once projectile breakup becomes possible, the decrease in the transmission becomes more rapid.

There is a close a relationship between the data shown in Figs. 3, 5, and 8 through the expression $Q_g = B_2 - B_{12}$, where B_2 is the binding of C_2 in V_2, and B_{12} is the binding of C_2 to C_1 through V_{12}; for Figs. 3 and 5 B_{12} is fixed at 4.22 MeV, and for Fig. 8, B_2 is fixed at 5.5 MeV. By using this expression, and curves fitted to the data in Figs. 3, 5, and 8, a common presentation can be made; this is shown in Fig. 9 for a projectile kinetic energy of 2.5 MeV.

From Fig. 9 it can be seen that there is a substantial difference between the probability behavior with increasing Q_g if this increase arises from deeper binding of C_2 in V_2 or through weaker binding of the projectile. If the increase in Q_g arises from deeper binding of C_2 in V_2, then with increasing Q_g the

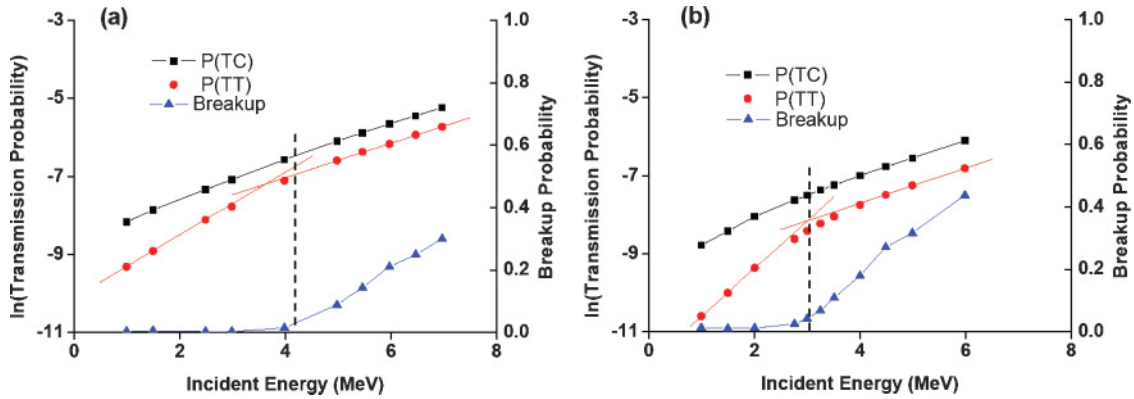

FIG. 7. (Color online) Transmission probabilities as a function of projectile energy for two projectile binding energies; (a) binding energy = 4.22 MeV, (b) 3.0 MeV; the vertical lines are at these values.

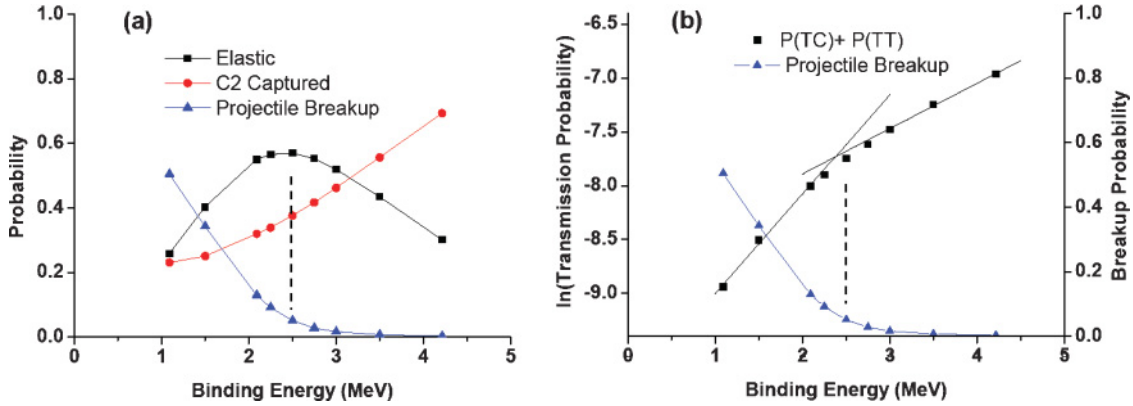

FIG. 8. (Color online) (a) Elastic, C_2 capture, and breakup probabilities as a function of projectile binding energy at a fixed projectile kinetic energy of 2.5 MeV; (b) C_1 transmission and breakup probabilities; the straight lines indicate the change in slope at ∼2.5 MeV. Both figures correspond to a fixed projectile energy of 2.5 MeV; the vertical lines are set at this energy.

elastic scattering probability and transmission $P(\mathrm{TT})+P(\mathrm{TC})$ increases monotonically, while the C_2 capture decreases. However, if the increase in Q_g is the result of reduced binding of the projectile, then the capture probability decreases more rapidly, the elastic probability peaks and then decreases, while the transmission probability decreases monotonically. So this finding demonstrates that the Q_g value alone is not necessarily a complete guide to reaction outcome.

A further inspection of Fig. 9 shows that for the situation where the variation of Q_g is from changing B_{12}, the probability curves show feature changes at ∼3 MeV. These changes are most likely associated with projectile breakup since this becomes possible when Q_g>3 MeV. The behavior of the transmission probability through the barrier for the two situations shown in Fig. 9(c) is particularly interesting since they have opposite trends with increasing Q_g. A possible way to explain this behavior, which is based on a simple energy redistribution argument, is outlined below.

The separation distance at which the projectile will be significantly affected by the scattering potential $V_1 + V_2$ will be related to the projectile binding energy B_{12}, since this determines the spatial spread of the projectile's wave function. For the case where variation of Q_g arises from an increase in B_2, and the projectile is tightly bound, the projectile remains relatively unaffected until it closely interacts with V_2. This interaction can lead to a transfer of C_2 to V_2, with the balance of binding energy being transferred, through the coupling between C_1 and C_2, into an increase in the kinetic energy of C_1, so giving C_1 a greater ability to penetrate the barrier. This is essentially the argument put forward in Ref. [29]. For the case where variation of Q_g arises from a reduction of B_{12}, the projectile's internal structure will be substantially affected, becoming more spatially extended and more easily deformed by external interactions. However, deformation will result in a transfer of kinetic energy to potential energy and so reduce the ability of the projectile to penetrate the barrier. The effect of kinetic energy increase due to C_2 transfer would be operating still, but since there is now a reduced coupling between C_1 and C_2, the ability to transfer the binding energy of C_2 in V_2 to an increase in the kinetic energy of C_1 is reduced. The overall balance in this situation is seen to be [Fig. 9(b)] a decrease in transmission with increasing Q_g, leading to the conclusion

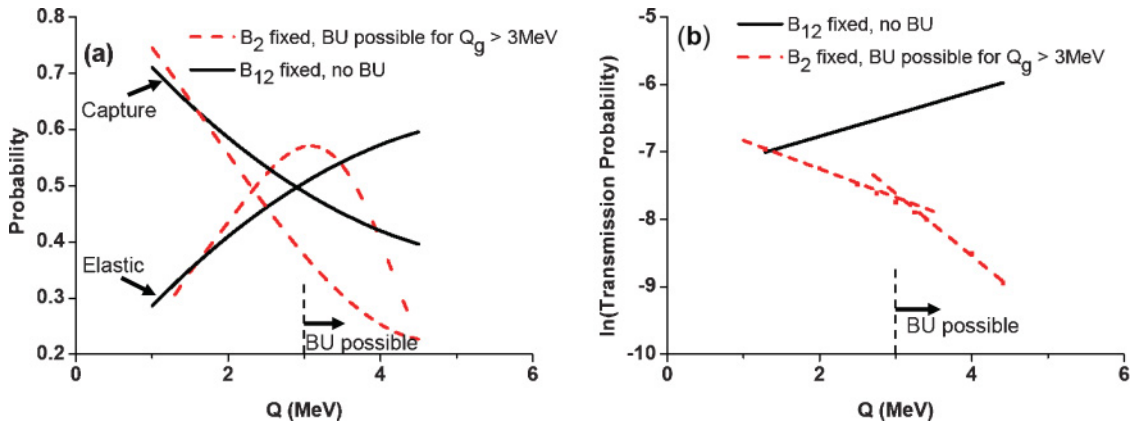

FIG. 9. (Color online) The solid and dashed curves are those that fit the data of Figs. 3, 5, and 8 for projectile kinetic energy E of 2.5 MeV. The elastic and capture probabilities are shown in (a), and the total transmission probability for C_1 is shown in (b). The dashed curves are for Q_g values determined by varying B_{12}, with B_2 fixed at 5.5 MeV. The solid curves are for Q_g determined by variation of B_2 with B_{12} fixed at 4.22 MeV; for this case projectile breakup, BU, is not possible.

that in this case the decreased coupling has more of an effect on the penetration of C_1 than the increase in available energy. The decrease in transmission becomes particularly noticeable if B_{12} is below the projectile kinetic energy E, which could be explained by noting that part of this energy will be lost to breakup (breakup is more likely to be irreversible than deformation, at least on the reaction time scale), so further reducing the ability of C_1 to penetrate the barrier, as seen in Fig. 9(b).

VI. STUDY CONCLUSIONS AND LINKAGE TO SUB-BARRIER NUCLEAR REACTIONS

A. Study summary

For the scattering situation diagrammatically represented in Fig. 1, this study has identified four main conclusions:

(i) All reaction processes are strongly influenced both by the binding of the projectile and by the binding of the projectile component C_2 within the attractive potential V_2. In particular, for low projectile energies, when these binding energies are equal, i.e., $Q_g = 0$, most of the final reaction flux resides in the channel where the projectile component C_2 is bound to V_2 with the other component C_1 reflected; in these situations the probability for elastic scattering of the projectile is small.

(ii) The transmission of the C_1 component through the barrier V_1 has a special significance at $Q_g = 0$, where there is equal probability that C_1 will be transmitted alone or attached to C_2. This behavior is observed irrespective of the projectile initial energy.

(iii) For variation of Q_g arising from different B_2 binding energies, the transmission of C_1 through the barrier V_1 varies approximately as $\exp(\alpha Q_g + \beta E)$, for a limited range of Q_g values greater than zero, where E is projectile kinetic energy and α and β are positive constants.

(iv) For those situations where the projectile kinetic energy is greater than its binding energy, breakup of the projectile, where the two components independently move away from the reaction site, becomes possible. It is found that the reaction flux in the other reaction channels is influenced significantly by the presence of the breakup channel.

(v) An increasing Q_g value is not necessarily accompanied by an increase in transmission, since if the Q_g increase is due to reduced projectile binding then transmission can be suppressed.

B. Linkage to nuclear tunneling

There are four main areas of interest concerning sub-Coulomb nuclear fusion reactions identified in the brief review at the beginning of this paper. The philosophy of the current work has been to study a model with limited degrees of freedom to determine if some of the issues of interest can be identified in such a model, and so to link them to a simple but general reaction mechanism. The potential system $V_1 + V_2$ of Fig. 1 has been studied as being representative of a fusion barrier that which permits processes such as scattering, absorption and breakup.

Conclusion (i) of Sec. VI A certainly has parallels with the nuclear situation, as matching of binding energies between participants of nuclear reactions (sometimes termed Q matching [45]) is a very important consideration when quantifying the strengths of various reaction outcomes. For example, in neutron-transfer reactions when angular momentum is not involved (i.e., $\ell = 0$ reactions), the transfers that are favored have $Q_g = 0$; this is the same general trend as displayed in Fig. 3.

Conclusion (ii) of Sec. VI A seems again to be related to Q matching. There is a mixing of the wave-function amplitudes for the neutral particle either to be attached to the potential V_2 or to V_{12}; this mixing leads to equal amplitudes at $Q_g = 0$. This behavior is common for a range of projectile energies. As discussed in Sec. V C, this effect can be related to shape polarization of the projectile and would be expected to occur at low energy and for weakly bound projectiles.

Conclusion (iii) of Sec. VI A again finds a parallel in sub-Coulomb reactions, and can be identified with the area of interest (iv) of Sec. I. As discussed by Zagrebaev [29], the fusion of the two charged cores can be enhanced by neutron transfer between the two approaching nuclei, as this increases the kinetic energy of the cores. In the paper it is proposed that the tunneling (fusion) probability, and hence fusion cross section, is increased by a factor of $\exp(\text{const} \times Q_g)$, where Q_g relates to the neutron transfer. The hypothesis of Zagrebaev therefore seems consistent with conclusion (iii), which holds when the increase in Q_g arises from an increase in B_2. Figure 5 shows the transmission probability for different Q_g values and projectile energies E; for the region above $Q_g = 0$, the logarithm of the transmission probability approximately varies linearly as suggested by Zagrebaev. This is suggestive that the physical process relevant to Fig. 5 is related to the transfer of nuclear binding energy into the kinetic energy of the projectile component penetrating the barrier. Indeed, inspection of the wave function in momentum space clearly shows this increase in momentum for C_1 as the Q_g value increases. However, the results of the current work, [conclusion (v) above] show that in other situations an increase in Q_g can result in a decrease in transmission.

Conclusion (iv) of Sec. VI A states that breakup of the projectile has a strong effect on the reaction outcome of other channels. Furthermore, the study shows that the breakup probability increases with increasing projectile energy and with decreasing projectile binding energy; the effect of breakup on the other reaction channels increases with breakup probability. These conclusions clearly have parallels with the actual nuclear situation as identified in the area of interest (iii) of Sec. I. In particular, when breakup of the projectile becomes possible, the current study shows that the transmission of the projectile through the barrier is suppressed.

The result identified in (v) of Sec. VI A has particular significance for the debate concerning the influence that projectile binding has on barrier transmission and therefore fusion.

Figure 9 clearly shows that if an increase in Q_g arises from stronger binding in the target system, then transmission increases. However, if an increase in Q_g comes from reduced projectile binding, then the transmission decreases. Furthermore, if the binding is reduced to a level that projectile breakup can occur, then the transmission probability decreases even more rapidly. In Sec. V D a simple energy argument was given to explain this difference of behavior. In addition, the decreasing transmission with decreasing binding energy is consistent with the theoretical analysis of Lee and Takigawa [43]. These authors demonstrate that for certain bound two-particle systems, incident on a barrier, which have internal wave functions which can respond quickly to external influences, then this interaction can lead to a reduction in the potential barrier, so leading to an increase in transmission relative to an inert system (i.e., one with a very large binding energy). This conclusion is consistent with other theoretical analysis, e.g., Ref. [21]. However, Lee and Takigawa also show that with weaker projectile binding a different process begins to emerge; the projectile energy levels become closer and therefore more readily populated, and so it becomes less likely that the excitation energy will be returned to the projectile kinetic energy—so leading to a reduction in transmission. It can be further speculated that if excitation into the breakup continuum becomes possible, then this would decrease further the transmission probability.

The study of nuclear reactions using radioactive beams is currently a very active research topic. One area of interest concerns the fusion reactions involving these radioactive nuclei, and in particular how the extended neutron tail affects the fusion process. If we can cautiously extend the conclusions of the present study to this particular nuclear situation, then these results suggest that there are two different Q_g regimes influencing fusion reactions between stable and weakly bound nuclei. First, for a transfer of a neutron from a particular neutron-rich nucleus to a series of stable nuclei corresponding to various positive Q_g, then it would be expected that the fusion probability would increase as $\exp(\alpha Q_g)$, where α is a positive constant. If, on the other hand, fusion of different weakly bound nuclei on a particular stable target are studied, then an increase of Q_g associated with more weakly bound nuclei would lead to a decrease in fusion, particularly so if breakup becomes possible. The existence of these two Q_g regimes may go some way to explain some of the difficulties of interpreting individual experimental results since which regime is appropriate will be sensitive to the individual parameters of the fusing nuclei.

In conclusion, it is interesting to see how a simple model with limited degrees of freedom shows characteristics similar to those observed in real fusion reactions which have many degrees of freedom. Q_g matching, shape polarization, transfer of binding energy to kinetic energy, and breakup effects all manifest themselves in a model with few degrees of freedom. This demonstrates that even for complex reactions, such as fusion, such models may be useful in providing some guidance to the most important processes that determine reaction outcome.

ACKNOWLEDGMENT

M.S. would like to acknowledge funding from Christ Church (Oxford, UK) and the Lindemann Trust.

[1] D. K. Roy, *Quantum Mechanical Tunneling and Its Applications* (World Scientific, Singapore, 1986).
[2] D. EcVault, *Quantum-Mechanical Tunneling in Biological Systems* (Cambridge University Press, Cambridge, UK, 1984).
[3] J. J. Kolata *et al.*, Phys. Rev. Lett. **81**, 4580 (1998).
[4] M. Trotta *et al.*, Phys. Rev. Lett. **84**, 2342 (2000).
[5] E. F. Aguilera *et al.*, Phys. Rev. Lett. **84**, 5058 (2000).
[6] Yu E. Penionzhkevich, V. I. Zagrebaev, S. M. Lukyanov, and R. Kalpakchieva, Phys. Rev. Lett. **96**, 162701 (2006).
[7] R. Raabe *et al.*, Nature (London) **431**, 823 (2004).
[8] S. M. Lukyanov *et al.*, Phys. Lett. B **670**, 321 (1990).
[9] C. Signorini *et al.*, Eur. Phys. J. A **2**, 227 (1998).
[10] C. Signorini *et al.*, Eur. Phys. J. A **5**, 7 (1999).
[11] C. Signorini *et al.*, Nucl. Phys. A **735**, 329 (2004).
[12] W. Loveland *et al.*, Phys. Rev. C **74**, 064609 (2006).
[13] J. Takahashi, M. Munhoz, E. M. Szanto, N. Carlin, N. Added, A. A. P. Suaide, M. M. deMoura, R. LiguoriNeto, A. SzantodeToledo, and L. F. Canto, Phys. Rev. Lett. **78**, 30 (1997).
[14] M. Dasgupta *et al.*, Phys. Rev. C **66**, 041602(R) (2002).
[15] P. K. Rath *et al.*, Phys. Rev. C **79**, 051601(R) (2009).
[16] M. Dasgupta *et al.*, Phys. Rev. Lett. **82**, 1395 (1999).
[17] L. F. Canto *et al.*, Nucl. Phys. A **821**, 51 (2009).
[18] M. S. Hussein, M. P. Pato, L. F. Canto, and R. Donangelo, Phys. Rev. C **46**, 377 (1992).
[19] N. Takigawa, M. Kuratani, and H. Sagawa, Phys. Rev. C **47**, R2470 (1993).
[20] M. S. Hussein, M. P. Pato, and A. F. R. de Toledo Piza, Phys. Rev. C **51**, 846 (1995).
[21] C. H. Dasso, S. Landowne, and A. Winther, Nucl. Phys. A **405**, 381 (1983).
[22] C. H. Dasso, S. Landowne, and A. Winther, Nucl. Phys. A **407**, 221 (1983).
[23] C. H. Dasso and A Vitturi, Phys. Rev. C **50**, R12 (1994).
[24] K. Hagino, A. Vitturi, C. H. Dasso, and S. M. Lenzi, Phys. Rev. C **61**, 037602 (2000).
[25] A. Diaz-torres and I. J. Thompson, Phys. Rev. C **65**, 024606 (2002).
[26] D. H. Dasso and A. Vitturi, J. Phys. G **31**, S1449 (2005).
[27] M. Ito *et al.*, Phys. Lett. B **637**, 53 (2006).
[28] A. C. Shotter, V. Rapp, T. Davinson, D. Branford, N. E. Sanderson, and M. A. Nagarajan, Phys. Rev. Lett. **53**, 1539 (1984).
[29] V. I. Zagrebaev, Phys. Rev. C **67**, 061601 (2003).
[30] Yu E. Penionzhkevich, V. I. Zagrebaev, S. M. Lukyanov, and R. Kalpakchieva, Phys. Rev. Lett. **96**, 162701 (2006).
[31] V. I. Zagrebaev, V. V. Samarin, and W. Greiner, Phys. Rev. C **75**, 035809 (2007).
[32] M. Trotta, A. M. Stefanini, L. Corradi, A. Gadea, F. Scarlassara, S. Beghini, and G. Montagnoli, Phys. Rev. C **65**, 011601 (2001).

[33] W. von Oertzen and Krouglov, Phys. Rev. **53**, R1061 (1996).
[34] M. Razavy, *Quantum theory of Tunneling* (World Scientific, Singapore, 2003).
[35] N. Saito and Y. Kayanuma, J. Phys. Condens. Matter, **6**, 3759 (1994).
[36] F. M. Pen'kov, Phys. Rev. A **62**, 044701 (2000).
[37] F. M. Pen'kov, J. Exp. Theor. Phys. **91**, 698 (2000).
[38] G. L. Goodvin and M. R. A. Shegelski, Phys. Rev. A **71**, 032719 (2005).
[39] G. L. Goodvin and M. R. A. Shegelski, Phys. Rev. A **72**, 042713 (2005).
[40] G. F. Bonini, A. G. Cohen, C. Rebbi, and V. A. Rubakov, Phys. Rev. D **60**, 076004 (1999).
[41] S. Bacca and H. Feldmeier, Phys. Rev. C **73**, 054608 (2006).
[42] C. A. Bertulani, V. V. Flambaum, and V. G. Zelevinsky, J. Phys. G **34**, 2289 (2007).
[43] S. Y. Lee and N. Takigawa, Phys. Rev. C **28**, 1123 (1983).
[44] K. Pruess and P. Lichtner, Nucl. Phys. A **291**, 475 (1977).
[45] G. R. Satchler, *Direct Nuclear Reactions* (Oxford University Press, Oxford, UK, 1981), p. 698.